Proposed Active Optical Frequency Standards based on Magneto-optical Trap Trapped Atoms

Wei Zhuang, Deshui Yu, Zhenhui Chen, Kaikai Huang, and Jingbiao Chen
School of Electronics Engineering & Computer Science, Peking University, Beijing 100871, P. R. China
e-mail: jbchen@pku.edu.cn

***Abstract*—A new conception of optical frequency standards, active optical frequency standards (AOFS) is under developing. In this report, we propose a novel scheme for active optical frequency standards based on magneto-optical trap (MOT) trapped atoms. With the advantages of 4-level atomic system proposed here, this scheme overcomes the main limitations on the accuracy of active optical clock based on atomic beam due to Doppler effect.**

I. INTRODUCTION

A new conception of optical frequency standards, active optical frequency standards (AOFS) has been proposed recently [1-5]. The advantages of AOFS based on optical lattice trapped atoms, thermal atomic beam, and laser slowed atomic beam have been considered [1-5]. An experimental setup of AOFS with thermal Ca beam [5] is under developing in Peking University.

In this report, we propose a novel scheme for active optical frequency standards based on magneto-optical trap (MOT) trapped atoms. With the advantages of 4-level atomic system proposed here, this scheme overcomes the main limitations on the accuracy of active optical clock based on atomic beam due to Doppler effect [1-5]. With laser cooled atoms, an AOFS can also reach high accuracy besides stability.

The potential lasing transitions of candidates of atom are listed in Table 1. Taking the Yb atom as an example, as shown in Fig.1, the proposed lasing transition is the 6s6p $^3P_2$ to 6s6p $^3P_1$, which has a wavelength of 5819 nm. In a 398.9nm blue MOT, some atoms are pumped to 6s7s $^3S_1$ state, and via fast decay, are accumulated on the 6s6p $^3P_2$ state since this state has 15s lifetime. Because the atom in 6s6p $^3P_1$ state has a lifetime much shorter than that of 6s6p $^3P_2$ state, the population inversion between 6s6p $^3P_2$ and 6s6p $^3P_1$ states is built up. Therefore the lasing transition can be coupled out via a laser cavity, and the output laser light can be used as an AOFS directly.

Clearly, the pumping lasers at 398.9 nm, 1311.2 nm wavelengths are far-detuned to the lasing transition at 5819 nm, thus the light shifts are suppressed dramatically. The detailed light-shift calculation, including blackbody radiation shift will appear elsewhere [6].

Supported by the National Key Basic Research and Development Programme of China under Grand No. 2005CB724500

In this report, we will present the result of calculations of dynamical process of population inversion, and lasing process with a Fabry-Perot type resonator.

TABLE I. POTENTIAL AOFS LASING TRANSITION PARAMETERS [7]

Atom	Transition From 6s6p $^3P_2$ State to 6s6p $^3P_1$ State		
	Wavelength(μm)	*Frequency(GHz)*	*Einstein Coefficient A(s^{-1})*
Mg	245.616	1221.42	9.106×10^{-7}
Ca	94.447	3176.40	1.612×10^{-5}
Sr	25.367	11826.4	8.266×10^{-4}
Yb	5.819	51551.4	6.848×10^{-2}

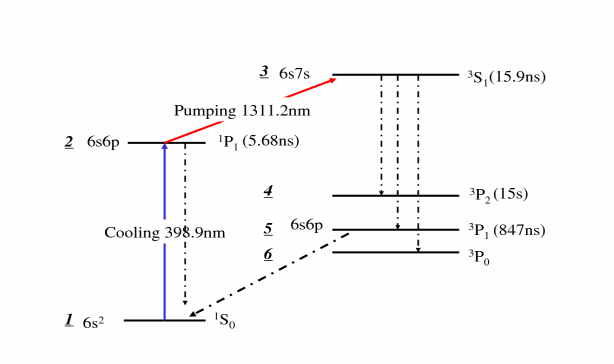

Figure 1. Partial energy diagram of Yb

II. POPULATION INVERSION OF TRAPPED ATOMS

Assuming that the atoms have been trapped in blue MOT with cooling light 398.9nm, parts of the trapped atoms would be pumped to upper state 6s6p $^1P_1$. Atoms can leave the trap through a number of mechanisms including collisions with the background gas atoms and decay from the 6s6p $^1P_1$ state into metastable states 6s6p $^3P_2$ and 6s6p $^3P_0$. The purpose of the pumping laser is to increase the transfer rate from the 6s6p $^1P_1$ state to 6s6p $^3P_2$ state with adjustable Rabi frequency of the pumping light 1311.2nm, which would make transition between the 6s6p $^1P_1$ state and 6s7s $^3S_1$ state as shown in

Fig.1. As a result, the atoms are accumulated in 6s6p $^3P_2$ and 6s6p $^3P_0$ states through the fast decaying from the 6s7s $^3S_1$ state. The population inversion could be formed between 6s6p $^3P_2$ and 6s6p $^3P_1$ states since there is a decaying passage from the lower state back to the 6s6p $^1S_0$ state. The whole process is clear after an approximate calculation in the following

Based on the theories of the interaction between the atoms and light, the density matrix equations for Yb atom interacting with the cooling light 398.9nm and the pumping light 1311.2nm are written in RWA-approximation as follows:

$$\frac{d\rho_{11}}{dt} = -2\Omega_{12}\rho_{12}^I + \Gamma_{21}\rho_{22} + \Gamma_{51}\rho_{55} + R_j - R_c\rho_{11}$$

$$\frac{d\rho_{22}}{dt} = 2\Omega_{12}\rho_{12}^I - 2\Omega_{23}\rho_{23}^I - \Gamma_{21}\rho_{22} - R_c\rho_{22}$$

$$\frac{d\rho_{33}}{dt} = 2\Omega_{23}\rho_{23}^I - (\Gamma_{34} + \Gamma_{35} + \Gamma_{36})\rho_{33} - R_e\rho_{33}$$

$$\frac{d\rho_{44}}{dt} = \Gamma_{34}\rho_{33} - R_e\rho_{44}$$

$$\frac{d\rho_{55}}{dt} = \Gamma_{35}\rho_{33} - \Gamma_{51}\rho_{55} - R_e\rho_{55}$$

$$\frac{d\rho_{12}^I}{dt} = \Omega_{12}(\rho_{11} - \rho_{22}) + \rho_{12}^R\Delta_1 + \Omega_{23}\rho_{13}^R - (\Gamma_{21}/2)\rho_{12}^I$$

$$\frac{d\rho_{12}^R}{dt} = -\rho_{12}^I\Delta_1 - \rho_{13}^I\Omega_{23} - (\Gamma_{21}/2)\rho_{12}^R$$

$$\frac{d\rho_{13}^I}{dt} = \rho_{13}^R(\Delta_1 + \Delta_2) + \rho_{12}^R\Omega_{23} - \rho_{23}^R\Omega_{12} - \frac{(\Gamma_{34} + \Gamma_{35} + \Gamma_{36})}{2}\rho_{13}^I$$

$$\frac{d\rho_{13}^R}{dt} = -\rho_{13}^I(\Delta_1 + \Delta_2) - \Omega_{23}\rho_{12}^I + \Omega_{12}\rho_{23}^I - \frac{(\Gamma_{34} + \Gamma_{35} + \Gamma_{36})}{2}\rho_{13}^R$$

$$\frac{d\rho_{23}^I}{dt} = \Omega_{23}(\rho_{22} - \rho_{33}) + \rho_{23}^R\Delta_2 - \Omega_{12}\rho_{13}^R - \frac{(\Gamma_{21} + \Gamma_{34} + \Gamma_{35} + \Gamma_{36})}{2}\rho_{23}^I$$

$$\frac{d\rho_{23}^R}{dt} = -\rho_{23}^I\Delta_2 + \Omega_{12}\rho_{13}^I - \frac{(\Gamma_{21} + \Gamma_{34} + \Gamma_{35} + \Gamma_{36})}{2}\rho_{23}^R$$

The subscript numbers of the density matrix correspond to different energy levels shown in Fig.1. Different from the conventional definition of the density matrix, here in above equations the diagonal elements mean the number of atoms in corresponding states and off-diagonal elements mean coherence for the total atoms. The Rabi frequency Ω_{12} associates with the product of electric dipole matrix d_{12} between the 6s6p $^1S_0$ state and 6s6p $^1P_1$ state and the electric strength ε_1 of the cooling light 398.9nm defined as $\Omega_{12}= d_{12}\varepsilon_1/2\hbar$, and $\Omega_{23}= d_{23}\varepsilon_2/2\hbar$, with electric dipole matrix d_{23} between the 6s6p $^1P_1$ state and 6s7s $^3S_1$ state and the electric strength ε_2 of the pumping light 1311.2nm. The values of Ω_{12}, Ω_{23} equal to $10^8 s^{-1}$ corresponding to the cooling light intensity 23.7mw/cm^2 and 5×10^7 s^{-1} corresponding to the pumping light 0.47 mw/cm^2 which are both lower than their saturated intensities. $\Delta_1=\omega_{21}-\omega_1$ and $\Delta_2=\omega_{32}-\omega_2$ are frequencies detuning of cooling and pumping light on the transition frequency which are set to 30MHz and 0 separately. Γ_{21}, Γ_{51}, Γ_{34}, Γ_{35}, Γ_{36} are decaying rates related to the lifetimes described in Fig.1. Moreover, considering the atoms escaping from the trapping MOT, the additional decaying rates of some states are expressed by R_e in the above equations, which is approximated to 250 s^{-1} by the size of the trapped

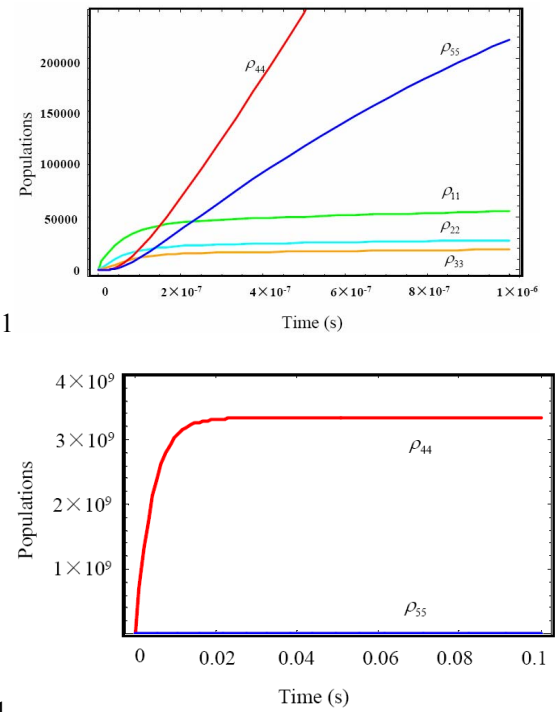

Figure 2. The dynamical populations with a pumping laser.

atoms cooled to Doppler Cooling Limit and the escaping velocity. R_j stands for the capture rate of MOT and R_c is introduced for the loss rate due to the collisions with background gas atoms measured as 0.36s^{-1} in experiments [8].

The numerical solutions of the above equations are shown in Fig.2 where the time range is confined to 0.1 s. The population inversion between 6s6p $^3P_2$ and 6s6p $^3P_1$ states, (ρ_{44}-ρ_{55}) is built up at time scale of 0.1 s. From Fig.2, it is obvious that once there are atoms in the 6s6p $^1S_0$ state, with the help of pumping laser the populations would transfer into metastable state in a high rate and the population inversion is built up between 6s6p $^3P_2$ and 6s6p $^3P_1$ states described as red and blue lines in the figure. There are no populations distributed elsewhere in a steady state except another metastable state 6s6p $^3P_0$ which hasn't been considered in the density matrix equations and would decrease the number of trapped atoms. However, it is known that the blue MOT would capture more and more "new" atoms which would compensate this decay mechanism and provides atoms transferred to the 6s6p $^3P_2$ state that we are interested in.

III. LASING OF ACTIVE OPTICAL FREQUENCY STANDARD

Now that there is population inversion in the trapped atoms, an optical resonant cavity could be applied to detect the probability of lasing transition between the inverted states. According to the classical laser theory, the oscillating process could start up once the optical gain exceeding the loss rate.

In the Russell-Saunders LS approximation the magnetic dipole moment μ for the 6s6p $^3P_2$ - 6s6p $^3P_1$ (Δm_j=0) transition is$(1/3)^{1/2}$ μ_B, where μ_B is the Bohr magneton [9]. We propose

to utilize a Fabry-Perot type resonator with mode volume about 10^{-7} $m^3$and cavity loss rate Γ_c about $2.7\times10^7 s^{-1}$ so that the laser emission coefficient is $K\sim g^2 t_{int}=6.6\times10^{-3}$ s^{-1} with g is atom-cavity coupling constant and t_{int} the interaction time. It should be noted that, the essential difference between normal laser and active optical frequency standard is laser cavity mode linewidth should be much larger lasing transition linewidth, which has been discussed carefully before [1-5]. Considering the accuracy correction, lasing of a 3-level atomic system [10-11] is not suitable for an active optical frequency since the light shift due to the pumping laser is un-tolerable for the accuracy requirement.

Then, the equations for emitted photons from the total atoms inside the cavity together with corresponding density matrix equations (for the total N atoms) are listed as follows:

$$\frac{d\rho_{11}}{dt}=-2\Omega_{12}\rho_{12}^{I}+\Gamma_{21}\rho_{22}+\Gamma_{51}\rho_{55}+R_j-R_c\rho_{11}$$
$$\frac{d\rho_{22}}{dt}=2\Omega_{12}\rho_{12}^{I}-2\Omega_{23}\rho_{23}^{I}-\Gamma_{21}\rho_{22}-R_c\rho_{22}$$
$$\frac{d\rho_{33}}{dt}=2\Omega_{23}\rho_{23}^{I}-(\Gamma_{34}+\Gamma_{35}+\Gamma_{36})\rho_{33}-R_e\rho_{33}$$
$$\frac{d\rho_{44}}{dt}=\Gamma_{34}\rho_{33}-R_e\rho_{44}-Kn\rho_{44}+Kn\rho_{55}$$
$$\frac{d\rho_{55}}{dt}=\Gamma_{35}\rho_{33}-\Gamma_{51}\rho_{55}-R_e\rho_{55}-Kn\rho_{55}+Kn\rho_{44}$$
$$\frac{dn}{dt}=Kn(\rho_{44}-\rho_{55})-\Gamma_c n$$
$$\frac{d\rho_{12}^{I}}{dt}=\Omega_{12}(\rho_{11}-\rho_{22})+\rho_{12}^{R}\Delta_1+\Omega_{23}\rho_{13}^{R}-(\Gamma_{21}/2)\rho_{12}^{I}$$
$$\frac{d\rho_{12}^{R}}{dt}=-\rho_{12}^{I}\Delta_1-\rho_{13}^{I}\Omega_{23}-(\Gamma_{21}/2)\rho_{12}^{R}$$
$$\frac{d\rho_{13}^{I}}{dt}=\rho_{13}^{R}(\Delta_1+\Delta_2)+\rho_{12}^{R}\Omega_{23}-\rho_{23}^{R}\Omega_{12}-\frac{(\Gamma_{34}+\Gamma_{35}+\Gamma_{36})}{2}\rho_{13}^{I}$$
$$\frac{d\rho_{13}^{R}}{dt}=-\rho_{13}^{I}(\Delta_1+\Delta_2)-\Omega_{23}\rho_{12}^{I}+\Omega_{12}\rho_{23}^{I}-\frac{(\Gamma_{34}+\Gamma_{35}+\Gamma_{36})}{2}\rho_{13}^{R}$$
$$\frac{d\rho_{23}^{I}}{dt}=\Omega_{23}(\rho_{22}-\rho_{33})+\rho_{23}^{R}\Delta_2-\Omega_{12}\rho_{13}^{R}-\frac{(\Gamma_{21}+\Gamma_{34}+\Gamma_{35}+\Gamma_{36})}{2}\rho_{23}^{I}$$
$$\frac{d\rho_{23}^{R}}{dt}=-\rho_{23}^{I}\Delta_2+\Omega_{12}\rho_{13}^{I}-\frac{(\Gamma_{21}+\Gamma_{34}+\Gamma_{35}+\Gamma_{36})}{2}\rho_{23}^{R}$$

Fig.3 and Fig.4 describe the solution for the photon numbers equation below and above threshold determined by the MOT capture rate, which tend to a steady-state value for sufficient time. Fig.5 shows that the steady photon number varies with the capture rate of MOT and the threshold phenomenon is exhibited just like traditional laser. We could conclude that a stable laser field is built up within laser cavity on condition that the population inversion is preserved. Compared with the traditional laser, the primary three conditions are also fulfilled for the AOFS based on magneto-optical trap trapped atoms just shown in this report, but the difference is that the lifetime for the lasing upper energy level is so long that the natural linewidth of the laser field is much narrower than the cavity mode linewith, which is 27 MHz

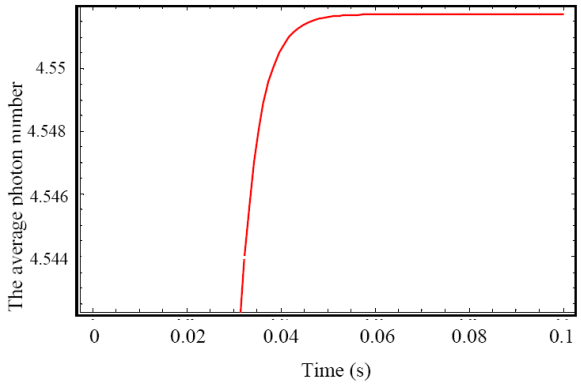

Figure 3. The average photon numbers inside the cavity below the threshold with the capture rate $R_j=10^{12}$atoms/second.

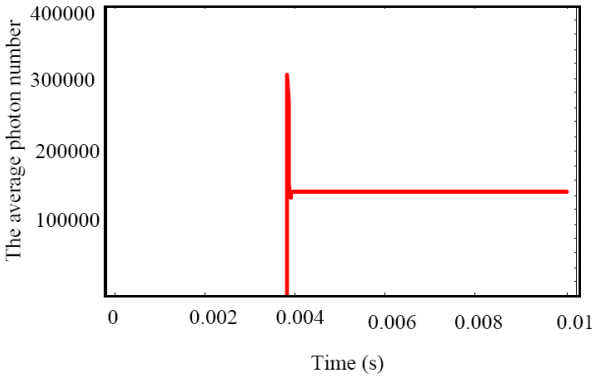

Figure 4. The average photon number inside the cavity above the threshold with the capture rate $R_j=2\times10^{12}$atoms/second.

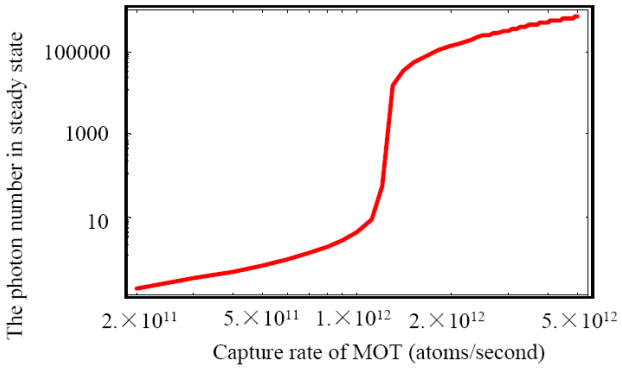

Figure 5. The steady photon numer as a function of the MOT capture rate.

assumed here. Furthermore, the temperature of cold atoms trapped in MOT decrease the broadening of the Doppler-effect-induced linewidth dramatically, therefore, it is suitable for AOFS with higher accuracy and better stability.

The underlying problem existing in this scheme is that the MOT magnetic field would induce energy level splitting through well-known Zeeman effect. In order to avoid the magnetic fluctuations to affect the frequency standard, 6s6p $^3P_2$ (m=0) and 6s6p $^3P_1$(m=0) are selected as laser energy level. The optical cavity should be placed 1-mm away from the MOT center where the magnetic field is large enough to

distinguish the Zeeman splitting induced σ transition, but small enough to ensure the three π transition [9] within the 250 Hz transit-time induced broadening linewidth of lasing gain.

From Fig. 5, the steady-state number of photons in laser cavity can reach 10,000 with the MOT capture rate of 2×10^{12} atoms/second. The output laser power will be 7.5×10^{-7} W. The quantum-limited linewidth of this bad cavity laser calculated by a modified Schawlow-Townes formula [2,12] is less than 10^{-3} Hz. Since the ratio $a = \Gamma_c / \Gamma_{gain} = 100$ here, the linewidth broadening of AOFS output laser due to cavity thermal noise [2,13] via cavity pulling effect can be as small as 2 mHz. The AOFS technique may provide a novel way for the long-coherence-time laser physics from 1-second time scale [3,14] to thousand-second coherence-time laser physics, besides other new optical clock mechanism [15]. It seems the main limitation will be the available intensive atomic flux and the MOT capture rate.

ACKNOWLEDGMENT

We thank Yiqiu Wang, Xuzong Chen, Hong Guo for helpful comments and suggestions on this topic. J. Chen thanks Tai Hyun Yoon for sending their manuscript [10] for reference.

REFERENCES

[1] J. Chen, X. Chen,"Optical Lattice Laser", Proc. of 2005 IEEE IFCS, pp608-610, 2005.

[2] J. Chen, "Active optical clock," arXiv:physics/0512096

[3] W. Zhuang, J. Chen, "Beyong One-Second Laser Coherence via Active Optical Atomic Clock", Proc. of EFTF 2006, pp373-375.

[4] W. Zhuang, D. Yu, and J. Chen, "Optical Clocks Based on Quantum Emitters", 2006 IEEE-IFCS, pp277-280.

[5] Z. Chen et al., "Proposed active optical frequency standard based on thermal Calcium beam",unpublished.

[6] W. Zhuang, J. Chen, "Light-shifts calculation of proposed active optical clock transitions," unpublished.

[7] http://physics.nist.gov/PhysRefData/Handbook/Tables

[8] R. Maruyama, Ph. D. Thesis, University of Washington, 2003.

[9] A. Godone and C. Novero, "The Magnesium frequency standard," Metrologia, vol. 30, pp.163-181, 1993.

[10] S. A. Pulkin, Tai Hyun Yoon, "Gain and lasing on forbidden transition in trapped atoms," private communication.

[11] Pulkin S.A., Uvarova S.V., E.E. Fradkin, Yu. I. Rozdestvenskii, Palchikov V.G., Ovsiannikov. "Gain and lasing on forbidden transitions in trapped atoms," Proc. of the 4th International Symp. MPLP2004, pp.308-314.

[12] S. J. M. Kuppens, M. P. van Exter, and J. P. Woerdman, "Quantum-Limited Linewidth of a Bad-Cavity Laser," Phys. Rev. Lett., vol. 72, pp.3815-3818, 1994.

[13] K. Numata, A. Kemery, and J. Camp, "Thermal-Noise Limit in the Frequency Stabilization of Lasers with Rigid Cavities" Phys. Rev. Lett., vol. 93, p.250602, 2004.

[14] Martin M. Boyd, Tanya Zelevinsky, Andrew D. Ludlow, Seth M. Foreman, Sebastian Blatt, Tetsuya Ido, Jun Ye "Optical Atomic Coherence at the 1-Second Time Scale," Science, vol. 314, pp. 1430 – 1433, 2006.

[15] Deshui Yu and Jingbiao Chen, "Optical Clock with Millihertz Linewidth Based on a Phas-Matching Effect", Phys. Rev. Lett., vol. 98, p.050801,2007.